



Lecture 13: Organization of Epithelial Tissue

Prof Dagmar Iber, PhD DPhil

MSc Computational Biology 2019/20

Contents

1 Organization of Epithelial Tissue

2 Euler's Theorem - Average Neighbour Number

3 Driving Forces behind the Polygon Distribution

- Topological Models: Impact of Cell Division
- Tissue Mechanics

4 Inference of cellular properties from images

5 3D Organisation of Epithelia

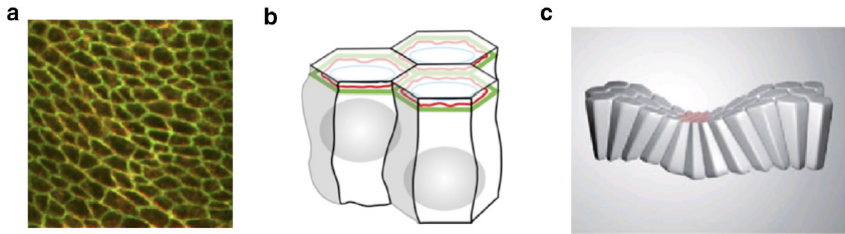
- Interkinetic Nuclear Migration (INM)

Organization of Epithelial Tissue

Organization of Epithelial Tissue

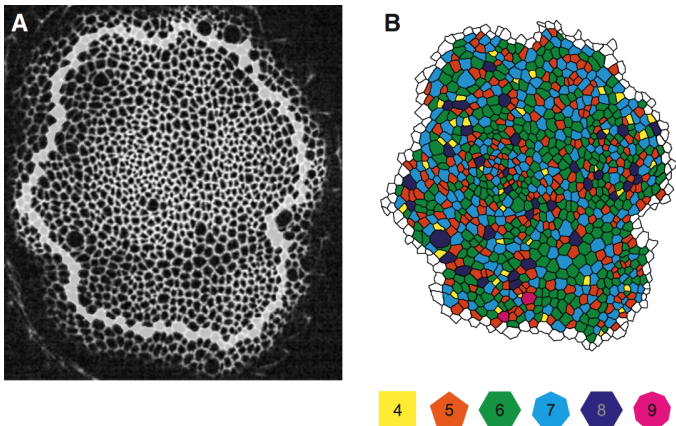
In an epithelium, each cell is tightly coupled to its neighbours by a ring of intercellular junctions which, in addition to maintaining the cohesion between cells, also forms a tight permeability barrier between cells.

The membrane boundaries of individual cells within an epithelium are, to a good approximation, polygonal in shape.



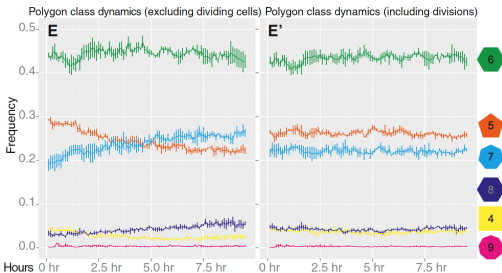
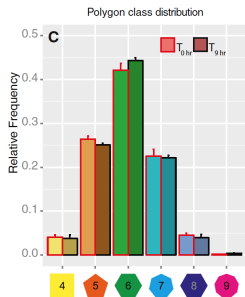
Apical Surface of the *Drosophila* Wing Disc Epithelium

Polygon



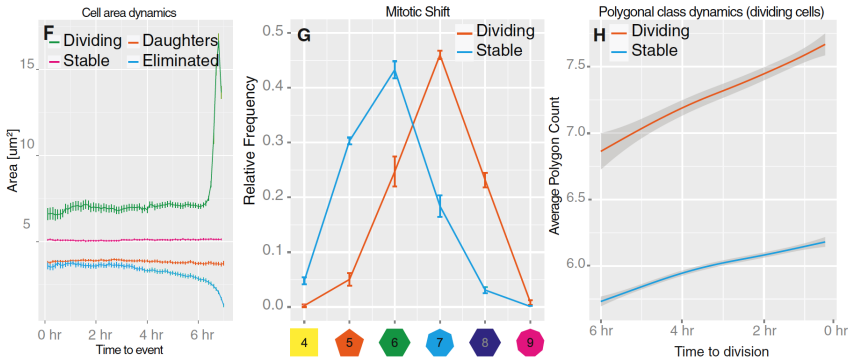
Drosophila Wing Disc: Heller, D., et al. (2016) Dev Cell 36, 103-116.

Polygon Distribution in the *Drosophila* Wing Disc



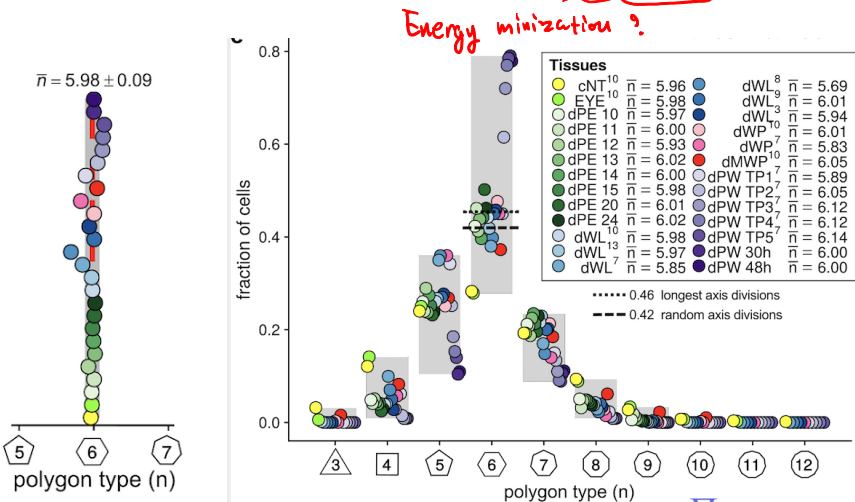
Heller, D., et al. (2016) Dev Cell 36, 103-116.

Edge Number increases during Cell Cycle



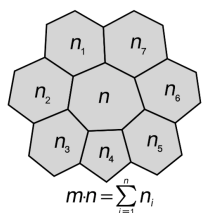
Heller, D., et al. (2016) Dev Cell 36, 103-116.

Epithelial cells have on average 6 neighbours



Aboav-Weaire's Law: Properties of Neighbours

Aboav-Weaire's Law (1970)

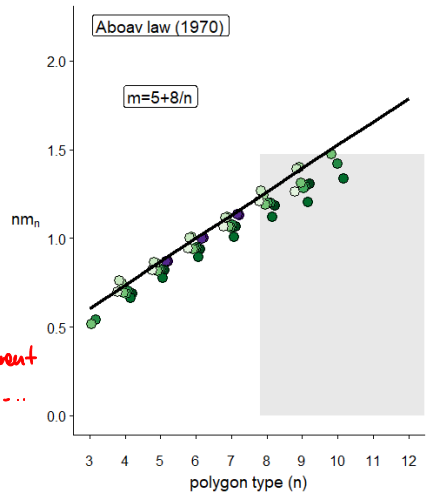


Average number of
neighbours of
a polygon

$$m_n = 5 + \frac{8}{n}$$

*, but it's different
from the hex...*

Aboav. The arrangement of grains in polycrystals.
Metallography 3, 383-390 (1970)



Average Cell Area related to Polygon class

Lewis' Law (1928)

$$A_n = \frac{A_0}{N} \frac{n - 2}{4}$$

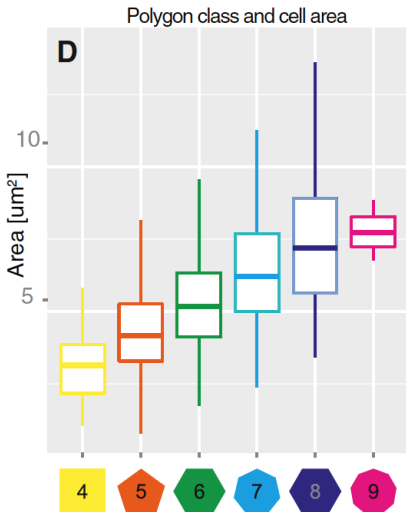
A_n average apical area

n number of its edges

N total number of cells

A_0 total tissue area.

Either one or both of N and A_0 can be time dependent, to account for growth and cellular division; yet the relationship is valid throughout the development of the tissue.



Euler's Theorem - Average Neighbour Number

Relation of the number of faces, edges & vertices

Every face, F_n , of a polygon with n sides has n edges. Every edge, E , separates two faces, F . In total,

$$\sum nF_n = 2E. \quad (1)$$

↓ no. of faces

Every edge joins two vertices and every vertex of connectivity α has α incident edges:

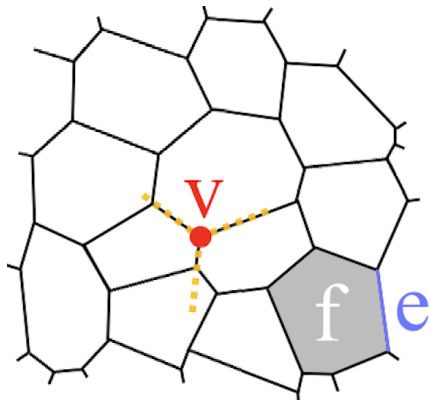
$\alpha=3$

$$\sum \alpha V_\alpha = 2E. \quad (2)$$

If on average α edges per vertex,

$$V = \frac{2}{\alpha} E. \quad (3)$$

vertex
edge



Euler's Theorem

The topological constraint follows from Euler's theorem relating the number of faces $F = N$, edges E and vertices V covering a two-dimensional manifold of Euler-Poincare characteristics χ ,

$$\textcircled{F} - E + V = \chi.$$

Faces

χ describes the global character of the manifold. For a sphere, $\chi = 2$.

Name	Image	Vertices V	Edges E	Faces F	Euler characteristic: $V - E + F$
Tetrahedron		4	6	4	2
Hexahedron or cube		8	12	6	2
Octahedron		6	12	8	2
Dodecahedron		20	30	12	2
Icosahedron		12	30	20	2

Wikipedia

https://en.wikipedia.org/wiki/Euler_characteristic

Constraint on Number of Faces

Using

$$E = \frac{1}{2} \sum nF_n; \quad V = \frac{2}{\alpha} E.$$

we obtain

$$\begin{aligned} F - E + V &= \chi \\ \Leftrightarrow F - E + \frac{2}{\alpha} E &= F + \frac{2 - \alpha}{\alpha} E = \chi \\ \Leftrightarrow F + \frac{2 - \alpha}{2\alpha} \sum nF_n &= \chi \end{aligned}$$

Average Neighbour Number

We further write for the fraction of cells with n neighbours,

$$p_n = \frac{F_n}{F} = \frac{N_n}{N} \quad (4)$$

and can then write

$$\sum n F_n = F \sum n p_n = F < n >. \quad (5)$$

Here, $< n >$ is the average number of neighbours.

Average Neighbour Number

$$\begin{aligned}
 F + \frac{2 - \alpha}{2\alpha} \sum nF_n &= \chi \\
 \Leftrightarrow F + \frac{2 - \alpha}{2\alpha} \langle n \rangle &= \chi \\
 \Leftrightarrow F + \frac{2 - \alpha}{2\alpha} F \langle n \rangle &= \chi \\
 \Leftrightarrow F \left(1 + \frac{2 - \alpha}{2\alpha} \langle n \rangle\right) &= \chi \\
 \Leftrightarrow \frac{2\alpha}{2 - \alpha} + \langle n \rangle &= \frac{2\alpha\chi}{(2 - \alpha)F} \\
 \Leftrightarrow \langle n \rangle &= \frac{2\alpha}{\alpha - 2} + \frac{2\alpha\chi}{(2 - \alpha)F}
 \end{aligned}$$

Limit of Large Tissues

$$\langle n \rangle = \frac{2\alpha}{\alpha - 2} + \frac{2\alpha\chi}{(2 - \alpha)F}$$

Unlike F , E and V , χ does not scale with the number of faces. For a large tissue, $\chi = O(1)$ is negligible in comparison with F such that

$$\lim_{F \rightarrow \infty} \frac{2\alpha\chi}{(2 - \alpha)F} = 0.$$

In the limit of large tissues we thus have

$$\langle n \rangle \approx \frac{2\alpha}{\alpha - 2}.$$

$\mathcal{M} F_n \rightarrow \infty$

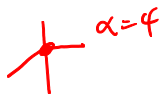
Average Number of Neighbours

$$\langle n \rangle \approx \frac{2\alpha}{\alpha - 2}$$



In a cellular mosaic, most vertices have three edges, i.e. $\alpha = 3$. Thus,

$$\langle n \rangle \approx \frac{2\alpha}{\alpha - 2} = 6.$$



Some tissues, have a low number of vertices with 4 edges. In the unrealistic case that $\alpha = 4$ for the entire tissue, we would have

$$\langle n \rangle \approx \frac{2\alpha}{\alpha - 2} = 4.$$

We thus expect that the average number of neighbours in tissues is close to 6, and certainly greater than 4.

Epithelial cells have on average 6 neighbours

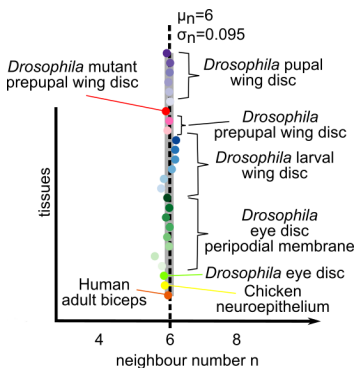
\Leftrightarrow each vertex has 3 edges
on average.

To minimize surface tension, cells tend to assume a spherical shape.

However, because of the tight cell-cell interactions, epithelial cells take on polygonal shapes.

Each cell would still minimize its individual surface tension by assuming a quasi-circular shape and thus a polygonal shape with very high edge number, n .

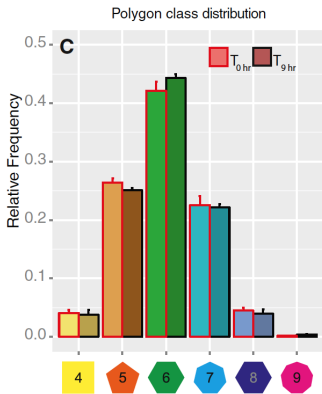
However, because of topological constraints $n \geq 6$. \Rightarrow each epithelial cell has on average six neighbours.



Driving Forces behind the Polygon Distribution

So what defines the distribution of the polygon types?

- 1 Impact of Cell Division (Gibson and co-workers)
- 2 Impact of Tissue Mechanics



Heller, D., et al. (2016) Dev Cell 36, 103-116.

Cell Topology, Geometry, and Morphogenesis in Proliferating Epithelia

Cellular geometry: specifies cell shape

Cellular topology: connectivity among cells in a tissue.

Manipulations that change cell shape, but maintain topology:
stretching or deforming a sheet of cells in such a way that the cells' respective shapes change, but all neighbor relationships are preserved.

Manipulations that change cell topology: processes such as perforation or tearing, in which cell contacts are broken, or convergent extension, in which cell contacts are both made and broken.

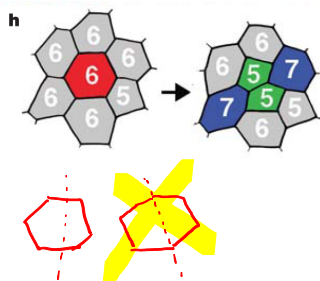
In epithelia, various elementary processes, such as cell division, cell rearrangement, and cell disappearance, modify cell sheet topology in stereotyped ways.

1. Impact of Cell Division

Impact of Cell Division (Gibson et al, 2006)

Model Assumptions:

- 1 cells are polygons with a minimum of four sides
- 2 cells do not re-sort
- 3 mitotic siblings retain a common junctional interface
- 4 cells have asynchronous but roughly uniform cell cycle times
- 5 cleavage planes always cut a side rather than a vertex of the mother polygon
- 6 mitotic cleavage orientation randomly distributes existing tricellular junctions to both daughter cells.



Gibson et al. Nature (2006).

Topological Model

In topological terms, each tricellular junction is a vertex, each cell side is an undirected edge, and each apical cell surface is a polygonal face.

- v_t : number of vertices after t divisions
- e_t : number of edges after t divisions
- f_t : number of faces after t divisions.

If we assume that cells divide at a uniform rate, then the number of faces (cells) will double after each round of division:

$$f_t = 2f_{t-1}$$

$$v_t = v_{t-1} + 2f_{t-1} \quad \text{each cell division results in } +2 \text{ vertices}$$

$$e_t = e_{t-1} + 3f_{t-1} \quad \text{each cell division results in } +3 \text{ edges}$$

Topological Model

Boundary effects become negligible for large t so that mean number of sites per cell can be determined as

$$s_t = \frac{2e_t}{f_t} = \frac{2(e_{t-1} + 3f_{t-1})}{2f_{t-1}} = \frac{s_{t-1}}{2} + 3 \quad (6)$$

This recurrence system leads to

$$s_t = 6 + 2^{-t}(s_0 - 6) \quad (7)$$

such that for

$$t \rightarrow \infty \quad s_t \rightarrow 6 \quad (8)$$

Topological Model

$$t \rightarrow \infty \quad s_t \rightarrow 6 \quad (9)$$

This implies that even in epithelia devoid of minimal packing, the system will assume a predominantly hexagonal topology as a consequence of cell division.

This behaviour is independent of cleavage plane orientation, and is instead a result of the formation of tricellular junctions.

Importantly, however, an average of six does not necessitate a prevalence (or even existence) of hexagons.

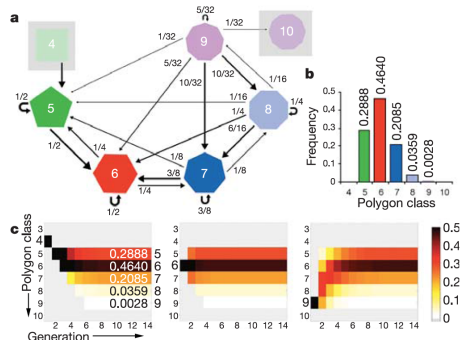
Markov chain model for the proliferation dynamics for polygonal cells.

- s : number of sides with $s > 3$
- p_s : relative frequency of s -sided cells in the population
- $\vec{p}^{(t)} = [p_4, p_5, p_6, p_7, p_8, p_9, \dots]$: system state at time t

The state dynamics is described by

$$\vec{p}^{(t+1)} = \vec{p}^{(t)} PS, \quad (10)$$

where P and S are probabilistic transition matrices.



Gibson et al. Nature (2006).

Markov chain model

$$\vec{p}^{(t+1)} = \vec{p}^{(t)}PS$$

The entries P_{ij} represent the probability that an i -sided cell will become j -sided after mitosis.

Matrix S : Topological arguments indicate that a cell will gain an average of one new side per cycle due to neighbour divisions.

P	Post-mitotic class						
	4	5	6	7	8	9	10
Pre-mitotic class	4	1					
5	1	1					
6	1	2	1				
7	1	3	3	1			
8	1	4	6	4	1		
9	1	5	10	10	5	1	
10							
...							

S	After neighbour divisions						
	4	5	6	7	8	9	10
Before neighbour divisions	4	0	1				
5	0	1					
6	0	1					
7	0	1					
8	0	1					
9	0	1					
10							
...							

neighbours
 getting
 1 more edge.

Probability that an i -sided cell will become j -sided after mitosis

- s_{t-1} sides (or junctions) at generation $t - 1$.
- K_t : random variable for the number of junctions distributed to one daughter cell on division at generation t , leaving $s_{t-1} - K_t$ for the other. No triangular cells are allowed / observed empirically

Assumptions:

- junctions are distributed uniformly at random around the mitotic cell
- the cleavage plane orientation is chosen uniformly at random (to bisect the rounded mitotic cell's area)

The (unnormalized) entries of P are the coefficients of Pascal's triangle.

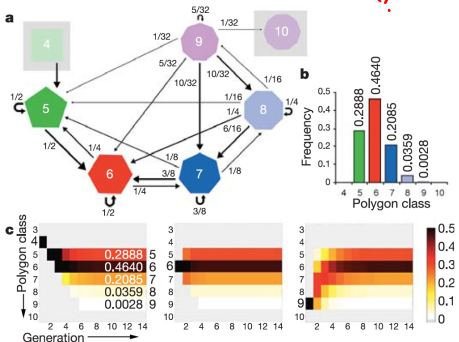
Markov chain model for the proliferation dynamics for polygonal cells.

steady state \leftarrow maybe due to the ergodic markov chain.
?

In equilibrium,

$$\vec{p}^{(t+1)} = \vec{p}^{(t)}$$

From this, one can obtain the equilibrium distribution to be approximately 28.9% pentagons, 46.4% hexagons, 20.8% heptagons and lesser frequencies of other polygon types.

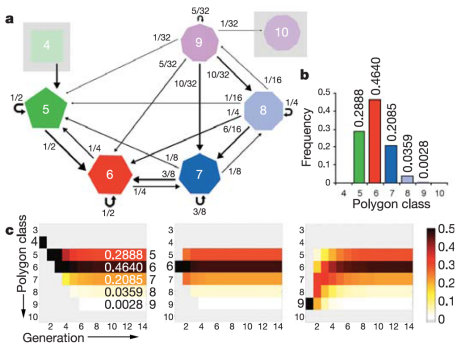


Gibson et al. Nature (2006).

Markov chain model for the proliferation dynamics for polygonal cells.

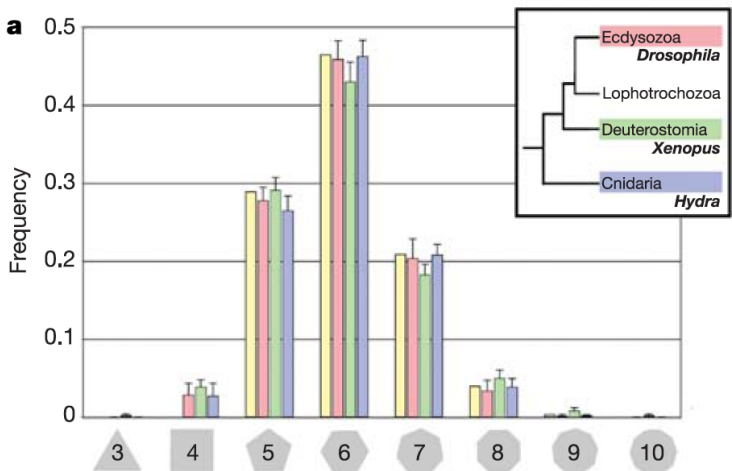
The model also predicts that the population of cells should approach this distribution at an exponential rate.

Consequently, global topology converges in less than eight generations, even for initial conditions where every cell is quadrilateral, hexagonal, or nonagonal.



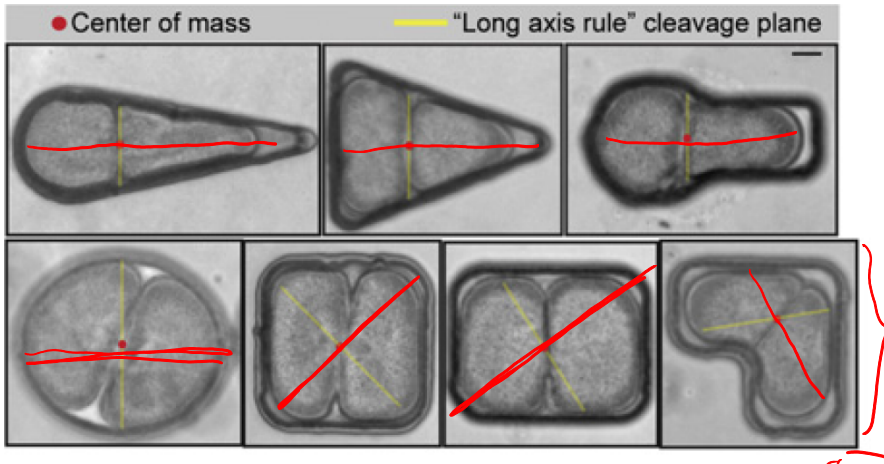
Gibson et al. Nature (2006).

Predicted and Observed polygon distributions.

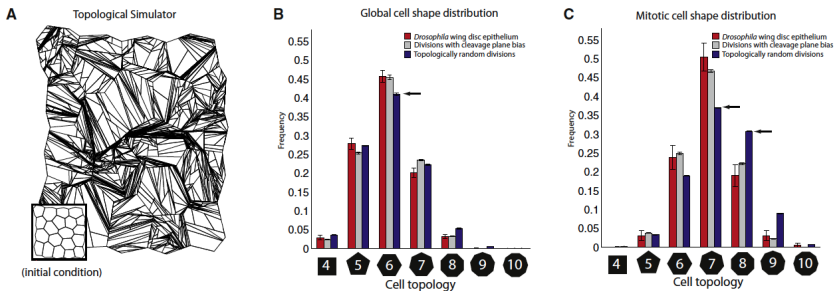


Cleavage Plane NOT random.

Hertwig's rule: division perpendicular to longest axis.

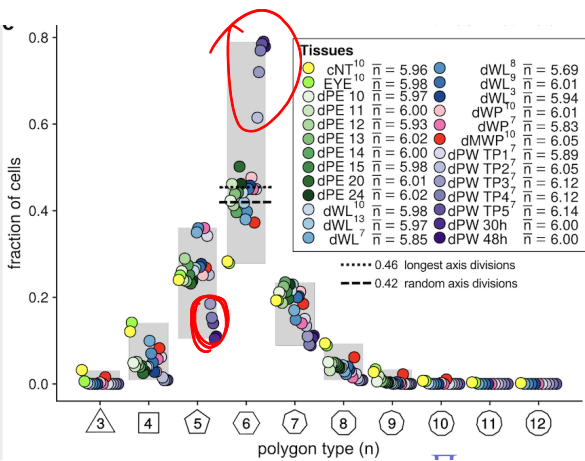


Better match of polygon distribution with division perpendicular to longest axis.



Gibson et al Cell (2011).

Different polygon distributions.



The fact that also other polygon distributions exist in nature than those predicted by the cell division-induced topological changes suggests that some other important aspect is still missing.

2. Tissue Mechanics

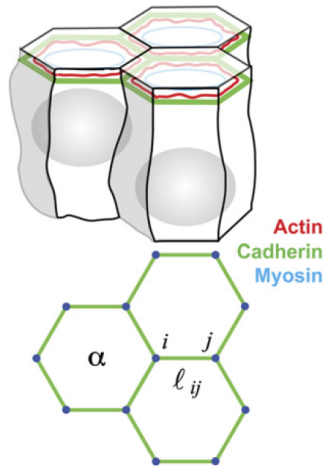
discussed last lecture

Modelling an epithelial sheet

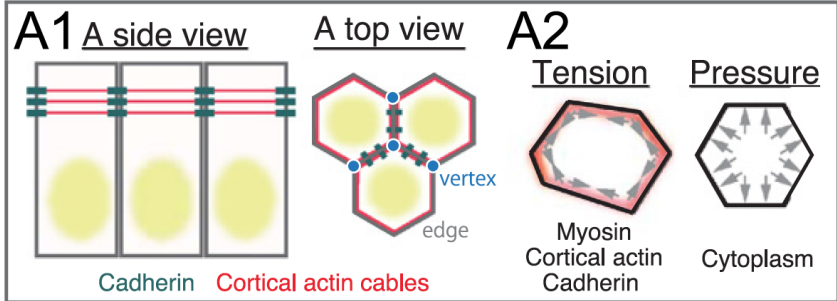
We will model an epithelium as a two-dimensional sheet of contiguous, coupled polygonal cells (i.e. as a collection of nodes connected by line segments).

We begin by describing a mechanical model for a single cell. To model an epithelium, it will then only be necessary to mechanically couple a suitable number of cells into a continuous two-dimensional sheet.

Further details in Weliky, M. and G. Oster (1990). Development 109: 373-386.



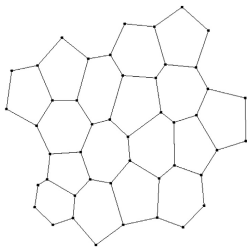
Modelling an epithelial sheet



Ishihara & Sugimura (2012) Theor Biol

Vertex Model

Representation of cells:



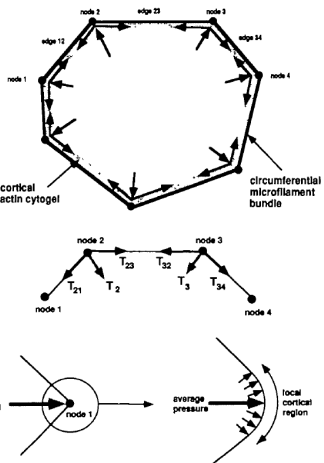
Fletcher et al., 2013

- cells represented by polygons
- neighboring cells share edges, intersection point = vertex

Elastic tension forces

The elastic tension forces at cell node, n , are represented by a pair of two-dimensional vectors, $\vec{T}_{(n,n-1)}$ and $\vec{T}_{(n,n+1)}$, applied to the node.

These vectors are directed along the line segments connecting this node to each of the two adjacent nodes, where $\vec{T}_{(n,n-1)}$ denotes the vector directed towards the node in the counterclockwise direction and $\vec{T}_{(n,n+1)}$ towards the clockwise node.



Hooke's Law

According to Hooke's law, the force \vec{F} needed to extend or compress a spring by some distance $\Delta \vec{x}$ is proportional to that distance. That is,

$$\vec{F} = k\Delta \vec{x}.$$

Elastic tension forces

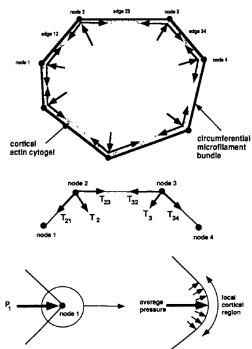
We will use the two-dimensional unit vectors $\vec{t}_{(n,n-1)}$ and $\vec{t}_{(n,n+1)}$ to describe the tension vectors' direction.

We can describe the elastic vector forces applied to each cell node as follows

$$\vec{T}_{(n,n+j)} = \vec{t}_{(n,n+j)} \cdot k_{elas} \cdot \Delta P$$

Here P is the cell perimeter, and k_{elas} is the elastic modulus of the cell cortex (i.e. the circumferential microfilament bundle and the cortical actin gel matrix).

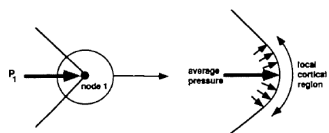
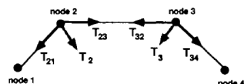
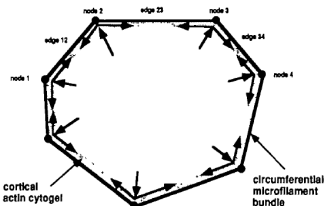
Larger values of k_{elas} reflect increasing contraction and/or density of microfilament bundles, while lower values reflect solation, which reduces the elastic modulus of the cortical actin gel matrix. Increasing the cell perimeter, P , stretches cortical fibers thus increasing their elastic restoring forces.



Pressure

Intracellular pressure is assumed to be uniform within the cell.

The pressure force at each node is represented by the two-dimensional vector \vec{P} directed outward from the cell boundary and bisecting the angle between the two line segments joined at a node; that is, the pressure acts normal to the polygonal surface at each node.

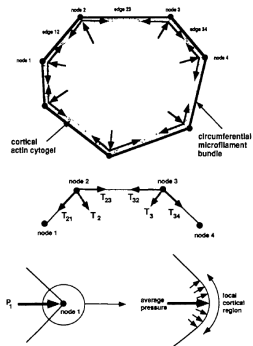


Pressure

The two-dimensional unit surface normal vector \vec{n} describes the direction of the nodal pressure.

The standard assumption is that a change in cell volume (surface area) results in a change in the osmotic pressure difference such that the pressure difference is inversely proportional to the volume (surface area, A_n):

$$\vec{P}_n = \frac{\text{const}}{A_n} \vec{n}$$



The net force at a node

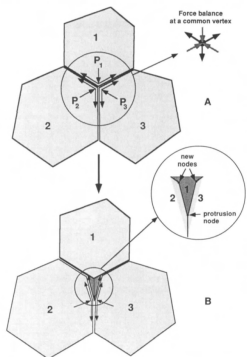
The net force acting at a cell node, n , is the vector sum of the nodal tensions and pressure:

$$\vec{F}_n = \vec{P}_n + \vec{T}_{(n,n-1)} + \vec{T}_{(n,n+1)}$$

The total force acting at an epithelial node is the sum of all net forces from all cells sharing this node plus the external forces:

$$\vec{F} = \sum_{n=1}^N \vec{F}_n + \vec{F}_{ext}$$

where N is the number of cells sharing the common junctional node.



Equations of Motion

The configuration of the model epithelium is specified by giving the location of each node.

Therefore, the **equations of motion** describing the changing configuration have the form

$$\mu \frac{d\vec{x}}{dt} = \vec{F}(x)$$

where μ is a viscous coefficient, \vec{x} is the position vector of the nodes, and $\vec{F}(x)$ is the vector of forces acting on the nodes.

Inertial forces are assumed to be negligible.

Equations of Motion

$$\mu \frac{d\vec{x}}{dt} = \vec{F}(x)$$

is a set of coupled differential equations where the number of equations is equal to the number of nodes in our simulation, which can be many hundreds. For the position vector of each node, \vec{x}_n , we have

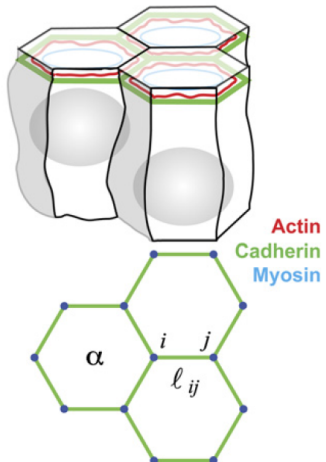
$$\mu \frac{d\vec{x}_n}{dt} = \sum_{n=1}^N \vec{P}_n + \vec{T}_{(n,n-1)} + \vec{T}_{(n,n+1)} + \vec{F}_{ext}$$

Since the equations are nonlinear, an analytical solution to this system is not possible, so we must apply numerical methods.

Energy Functional

Alternatively, we can use an energy functional and determine the steady state distribution:

$$E = \underbrace{\sum_{\langle i,j \rangle} \lambda_{i,j} l_{i,j}}_{\text{surface tension}} + \underbrace{\sum_{\alpha} \gamma_{\alpha} \Pi_{\alpha}^2}_{\text{cortical tension}} + \underbrace{\sum_i \kappa_{\alpha} (A - A_0)^2}_{\text{area elasticity}}$$



Relation between Forces and Energy-based View

Evolution in time:

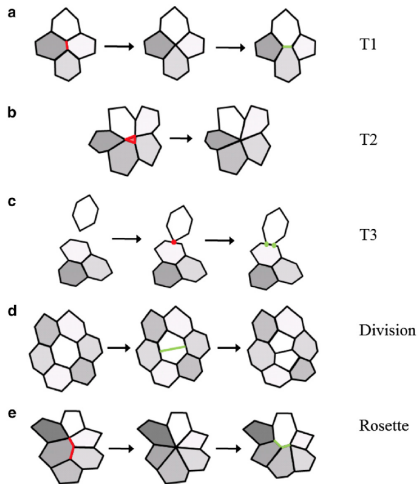
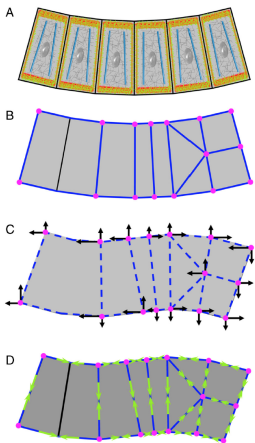
- vertex i moves according to: $\mu \frac{d\mathbf{x}_i}{dt} = \mathbf{F}_i$
- forces derived from energy potentials:

$$\mathbf{F}_i = \frac{\partial E}{\partial \mathbf{R}_i}$$

$$E(\mathbf{R}_i) = \sum_{\alpha} \frac{K_{\alpha}}{2} (A_{\alpha} - A_0)^2 + \sum_{<i,j>} \frac{\Gamma_{ij}}{2} (r_{ij} - l_{ij})^2$$

- term 1: area elasticity, K_{α} = elasticity coefficient
- term 2: perimeter contractility, Γ_{ij} = contractility coefficient

Junctional Rearrangement

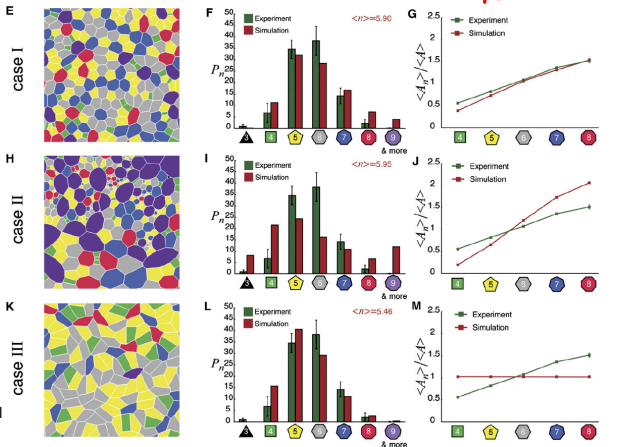
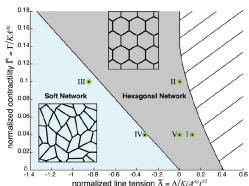


Brodland, G. W., et al. (2010) PNAS 107: 22111-22116.

Fletcher, A. G., et al. (2014). Biophys J 106: 2291-2304.

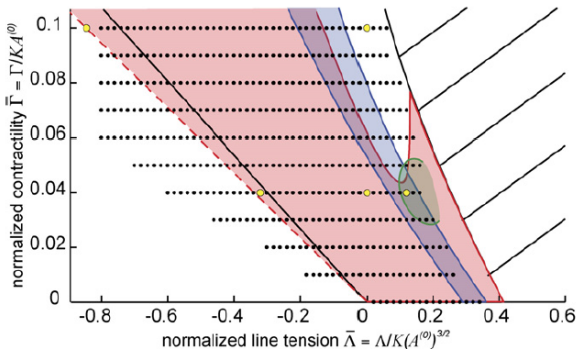
Vertex Model of epithelial sheet

Membrane Tension versus Cell Junction Strength



Farhadifar, R., et al. (2007). Curr Biol

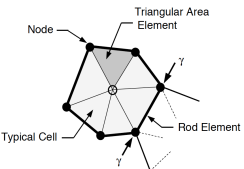
Comparison to Wing Disc Data



same polygon distribution
same area distribution
same response to laser ablation *Lauz's law*

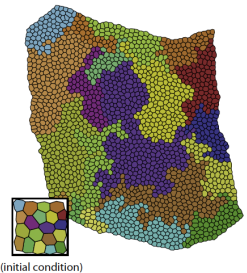
FEM Tissue Simulations & longest axis division

Better match of polygon distribution with division perpendicular to longest axis.

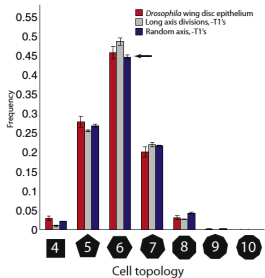


Gibson et al Cell (2011).

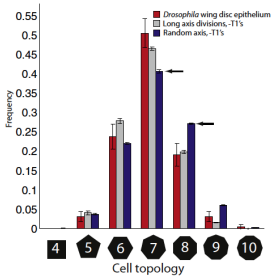
D Finite element simulator



E Global cell shape distribution



F Mitotic cell shape distribution



Conclusion

Both tissue mechanics and the cell division angle determine the polygon distribution in epithelia.

Summary

emerges because of the areas ← division cell area threshold

Properties of Epithelia:

- $< n > = 6$ (Euler's Theorem - Topological Argument)
- Polygon Distribution: Cell Division Angle & Tissue Mechanics
- Lewis' Law: $A_n = \frac{A_0}{4N}(n - 2)$ (??) all the epithelial cells follows
- Aboav-Weaire's Law: $m_n = 5 + \frac{8}{n}$ (??) angle adds up to 360° at vertex

$$E = \sum \lambda_{ij} I_{ij} + \sum_a \frac{r_a}{2} \pi^2 \Rightarrow$$

Energy minimization is driving the no. of hexagons [If] the cell area remains the same

With $\sum (A - A_0)^2$ cells with few  has smaller Area



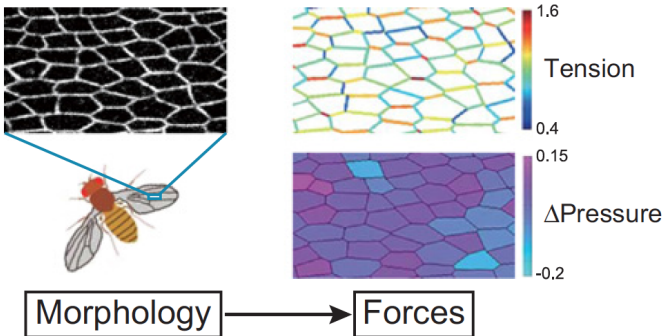
has larger Area.

Lewis's law would force the edges here smaller length?

Inference of cellular properties from images

Inference of cellular properties from images

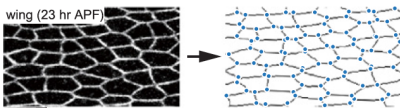
Estimating the dynamics of forces



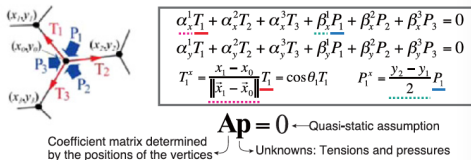
Ishihara, S. & Sugimura, K. (2012) Bayesian inference of force dynamics during morphogenesis. J Theor Biol 313, 201-211

Inference of cellular properties from images

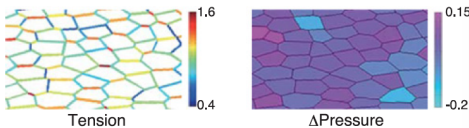
B1 Input: an image of cells (positions of vertices)



B2 Balance of forces at each vertex



B3 Output: relative values of tension and pressure



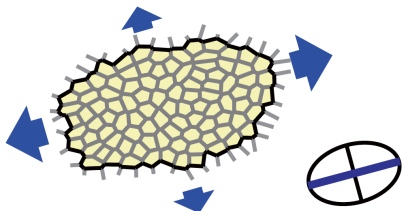
Ishihara, S. & Sugimura, K. (2012) Bayesian inference of force dynamics during morphogenesis. J Theor Biol 313, 201-211

Batchelor Stress Tensor

$$\sigma = \frac{1}{A} \left(- \sum_i P_i A_i \mathbf{I} + \sum_{[ij]} T_{ij} \frac{\mathbf{r}_{ij} \otimes \mathbf{r}_{ij}}{|\mathbf{r}_{ij}|} \right) \quad (11)$$

where \mathbf{I} is the two-dimensional identity matrix and $A = \sum_i A_i$ is the total tissue area.

Note that the scale of σ is undetermined. But quantities like the maximal stress direction can be obtained.

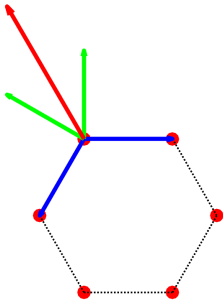


$$N_{xx} = \left[- \sum_{cell:i} \Delta P_i A_i + \sum_{edge:j} T_j \frac{\Delta x_j \Delta x_j}{|\Delta \vec{x}_j|} \right] \Bigg/ \sum_{cell:i} A_i$$

$$N_{yy} = \left[- \sum_{cell:i} \Delta P_i A_i + \sum_{edge:j} T_j \frac{\Delta y_j \Delta y_j}{|\Delta \vec{x}_j|} \right] \Bigg/ \sum_{cell:i} A_i$$

$$N_{xy} = N_{yx} = \left[\sum_{edge:j} T_j \frac{\Delta x_j \Delta y_j}{|\Delta \vec{x}_j|} \right] \Bigg/ \sum_{cell:i} A_i$$

Forces acting at a given node



$\vec{r}_i^\perp = (-y_i, x_i)$:
orthogonal vector

- $\vec{r}_i = (x_i, y_i)$: positions of vertices
- T_{ij} : tension of the vertex that connects the i -th and j -th vertices
- P_i : pressure of the i -th cell

$$\begin{aligned} \vec{F} = & \frac{\vec{r}_2 - \vec{r}_1}{\|\vec{r}_2 - \vec{r}_1\|} T_1 + \frac{\vec{r}_6 - \vec{r}_1}{\|\vec{r}_6 - \vec{r}_1\|} T_6 \\ & + \frac{1}{2} \left(\frac{[\vec{r}_2 - \vec{r}_1]^\perp}{\|\vec{r}_2 - \vec{r}_1\|} \|\vec{r}_2 - \vec{r}_1\| (P_1 - P_0) \right) \\ & + \frac{1}{2} \left(\frac{[\vec{r}_1 - \vec{r}_6]^\perp}{\|\vec{r}_1 - \vec{r}_6\|} \|\vec{r}_1 - \vec{r}_6\| (P_1 - P_0) \right) \end{aligned}$$

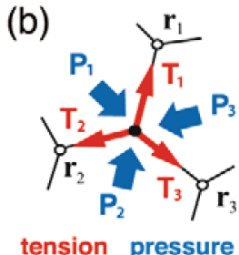
Forces: component notation

- $r_i = (x_i, y_i)$: positions of vertices
- T_{ij} : tension of the vertex that connects the i -th and j -th vertices
- P_i : pressure of the i -th cell

Let us consider the force acting on the 0-th vertex at the origin $r_0 = (0, 0)$. The forces in the x and y directions are given by

$$F_0^x = \sum_{i=1}^3 \frac{x_i}{|\vec{r}_i|} T_i - \sum_{i=1}^3 \frac{y_i}{2} (P_i - P_{i+1})$$

$$F_0^y = \sum_{i=1}^3 \frac{y_i}{|\vec{r}_i|} T_i + \sum_{i=1}^3 \frac{x_i}{2} (P_i - P_{i+1})$$



Ishihara, S. et al. (2013) The European physical journal. E, Soft matter 36, 9859

Forces: component notation

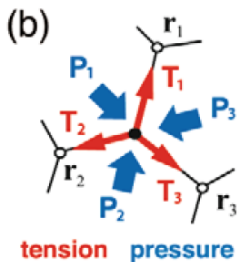
$$F_0^x = \sum_{i=1}^3 \frac{x_i}{|\vec{r}_i|} T_i - \sum_{i=1}^3 \frac{y_i}{2} (P_i - P_{i+1})$$

$$F_0^y = \sum_{i=1}^3 \frac{y_i}{|\vec{r}_i|} T_i + \sum_{i=1}^3 \frac{x_i}{2} (P_i - P_{i+1})$$

Orientation of the edge: $\theta_{ij} = \tan^{-1} \left(\frac{y_{ij}}{x_{ij}} \right)$

$$\Rightarrow \frac{x_i}{|\vec{r}_i|} = \cos(\theta_{ij}); \quad \frac{y_i}{|\vec{r}_i|} = \sin(\theta_{ij})$$

Pressures act along the sides of the cells in their normal direction. Projection to the x - and y -axes gives the pre-factors $-y_i$ and x_i , respectively, of the normal force. Half of the force acts on each end-point.



Ishihara, S. et al. (2013) The European physical journal. E, Soft matter 36, 9859

Full system of Equations

Repeating the same derivation of force-balance equations for every vertex, we obtain a vector

$$\vec{F} = (\vec{F^x}, \vec{F^y})^T \quad (12)$$

that represents the forces acting on vertices in the x and y directions as

$$\vec{F} = \mathbf{A_T} \vec{T} + \mathbf{A_P} \vec{P} = \mathbf{A} \vec{X}. \quad (13)$$

Here, \vec{T} and \vec{P} are column vectors composed of T_{ij} and P_i , respectively. $\vec{X} = (\vec{T}, \vec{P})^T$ represents the unknown variables to be inferred. $\mathbf{A_T}$ and $\mathbf{A_P}$ represent matrices with the coefficients of T_{ij} and P_i .

Dimension of Full system of Equations

$$\vec{F} = \mathbf{A}_T \vec{T} + \mathbf{A}_P \vec{P} = \mathbf{A} \vec{X}.$$

Suppose we have an image, in which N cells are surrounded by R cells:

- E : numbers of cell contact surfaces (edges)
- V : number of vertices

Dimensions

- \vec{T} : $[E \times 1]$, \vec{P} : $[N + R \times 1]$, \vec{X} : $[E + N + R \times 1]$
- \vec{F} : $[2V \times 1]$
- \mathbf{A}_T : $2V \times E$, \mathbf{A}_P : $[2V \times (N + R)]$, \mathbf{A} : $[2V \times (E + N + R)]$

Quasi-steady State Assumption

Under the assumption of quasi-static cell shape changes, the force-balance equation becomes

$$\vec{F} = \mathbf{A}_T \vec{T} + \mathbf{A}_P \vec{P} = \mathbf{A} \vec{X} = 0 \quad (14)$$

This gives us a relationship between the observable geometry (angles and lengths) of cells and the unknown tensions \vec{T} and pressures \vec{P} to be determined.

Note that we can only determine **relative forces** and **pressure differences**.

Overdetermined System

$$\vec{F} = \mathbf{A}_T \vec{T} + \mathbf{A}_P \vec{P} = \mathbf{A} \vec{X} = 0 \quad (15)$$

Number of unknowns = length of \vec{X} == number of cells ($N + R$) plus cell contact surfaces (E).

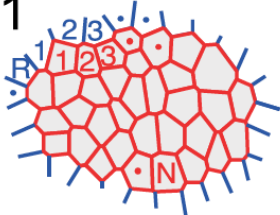
Number of conditions = $2 \times$ number of vertices

Number of unknowns is smaller than the number of the conditions for a sufficient number of cells.

To get plausible and unique estimates, the inverse problem must be formulated to handle this indefiniteness.

The Inverse Problem

C1

 $N + R$ cells $e + 2R$ edges

$$e = 3(v + f)/2 - f$$

$$v - e + N = 1$$

 $v + R$ vertices f four-way junctionsequality for e, v , and f

topological constraint

→ **$R + 1 + f$ indefiniteness**
(boundary + Phs + four-way j)

C2 Inverse problem

$$P(\mathbf{p}|\mathbf{b}) \propto P(\mathbf{b}|\mathbf{p}) \pi_T(\mathbf{p})$$

Posterior distribution

Likelihood

Prior

$$\exp\left[-\frac{1}{2\sigma^2}\|\mathbf{Ap} - \mathbf{b}\|^2\right]$$

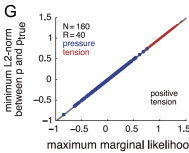
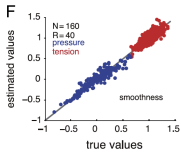
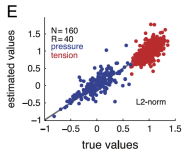
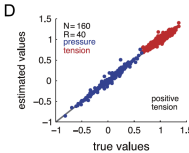
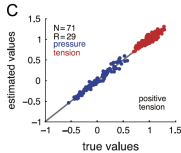
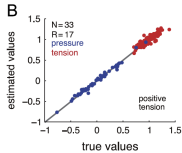
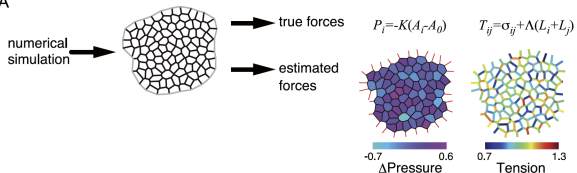
Force balance

$$\exp\left[-\frac{1}{2\omega^2}\sum_{[ij]}(T_{ij} - T_e)^2\right]$$

Positive tension

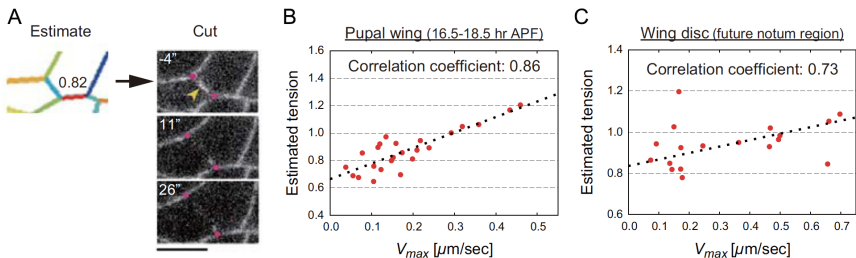
Estimated relative pressures and tensions against their true values

A



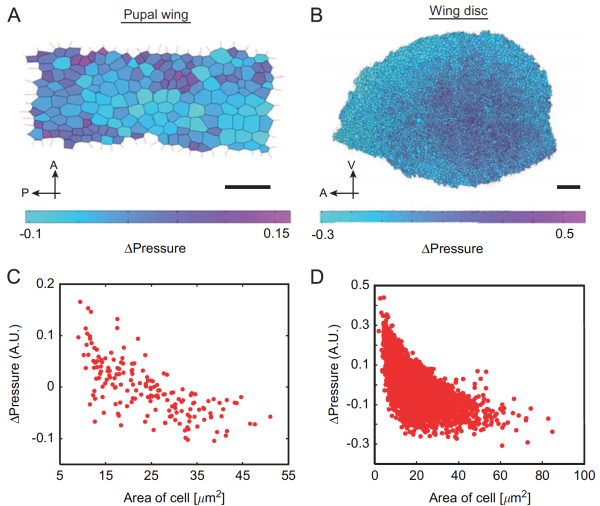
Ishihara, S. & Sugimura, K.
Bayesian inference of force dynamics during morphogenesis. J Theor Biol 313, 201-211,
doi:10.1016/j.jtbi.2012.08.017
(2012).

In vivo Validation



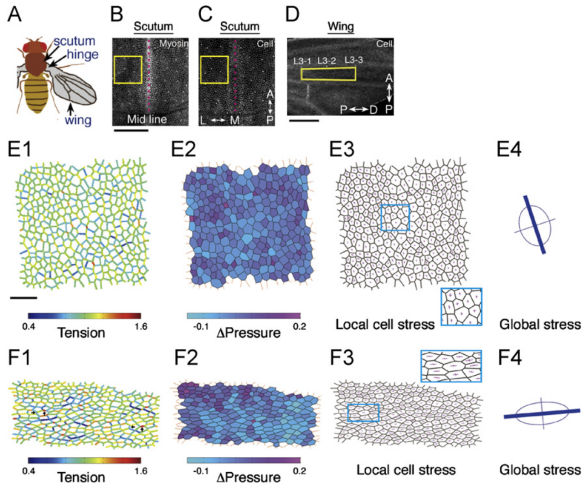
Ishihara, S. & Sugimura, K. Bayesian inference of force dynamics during morphogenesis. J Theor Biol 313, 201-211, doi:10.1016/j.jtbi.2012.08.017 (2012).

Inferred Pressure & Tension in the Wing Disc



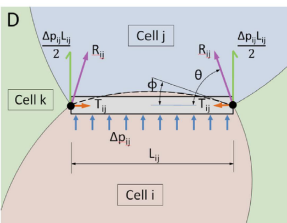
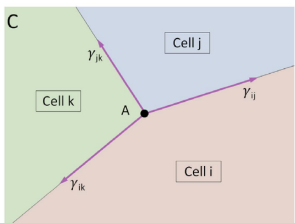
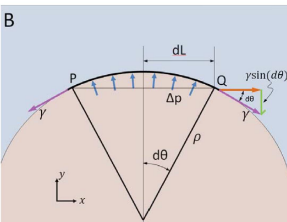
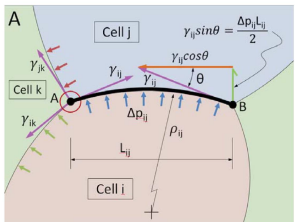
Ishihara, S. & Sugimura, K.
Bayesian inference of force dynamics
during morphogenesis. J Theor Biol
313, 201-211,
doi:10.1016/j.jtbi.2012.08.017
(2012).

Inferred Pressure & Tension in the Wing Disc



Ishihara, S. & Sugimura, K.
 Bayesian inference of force dynamics
 during morphogenesis. *J Theor Biol*
 313, 201-211,
 doi:10.1016/j.jtbi.2012.08.017
 (2012).

CELLFit: Segment also Curvature of Membranes



Laplace Equation:

$$\Delta p_{ij} = \frac{\gamma_{ij}}{\rho_{ij}} \quad (16)$$

ρ_{ij} : radius of curvature

γ_{ij} : tension

Brodland, G. W. et al (2014) Plos One

Summary

Inference of Epithelial Properties:

- Images of epithelia can be used to infer hydrostatic pressure and membrane tension
- Challenge to deal with overdetermined system and low quality data
- What is the correct model?

shrinkage is somewhat possible for spheres in 3D



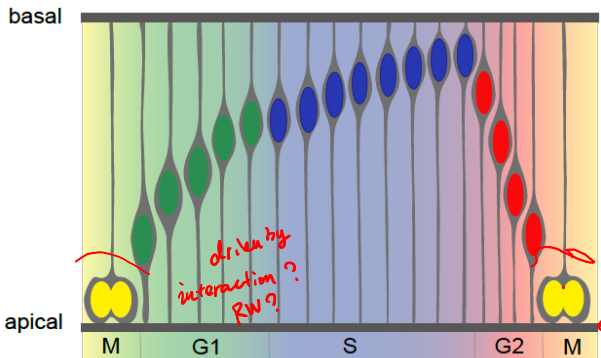
neighbour transition is essential for "shrinkage"

3D Organisation of Epithelia

Energy minimization is driving the "transition" along the dimension

Interkinetic Nuclear Migration (INM)

Interkinetic Nuclear Migration (INM)



Apical migration in G2 is driven by an apical force directed by dynein motors and microtubules.

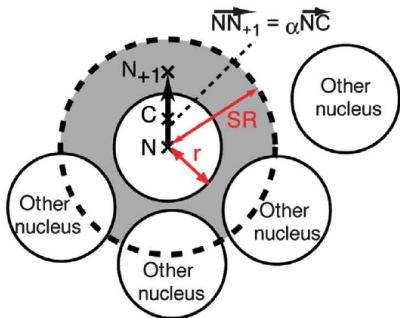
BD

What drives Nuclei Migration in G1?

- Active Transport?
- Crowding? geometry "passive" why?
- maybe MT and Actin in Apical.
 } Tension & RW
 } MT T Repulsion

Kosodo Model: Excluded Volume Effect

2D Model: nuclei represented by circles (radius $5\mu\text{m}$)



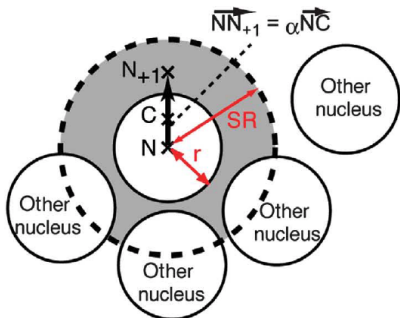
Kosodo et al (2011) EMBO

Time Stepping

For each nucleus

- draw a circle with search radius $SR = 10\mu\text{m}$ from the center of the nucleus, N ,
- calculate the centroid, C , of the area within this circle excluding the region occupied by nuclei (gray area)
- The vector \vec{NC} represents the direction and degree of nuclear movement.
- The new center of the nucleus, N_{+1} , is defined as $\vec{NN}_{+1} = \alpha \vec{NC}$
- $\alpha = 1$ coefficient for the degree of repulsion.
- After each step, the cell cycle phase of each nucleus progressed.

Kosodo Model: Excluded Volume Effect

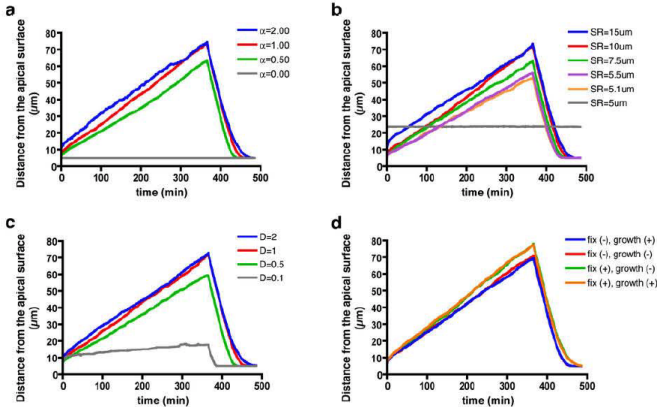


Initial Conditions

- Box size: $200\mu\text{m}$ wide; height $50\mu\text{m}$ high along the apical-to-basal axis.
- 200 nuclei were randomly positioned in the $200\mu\text{m}$ wide space (Density $D = 1$)
- The initial cell cycle phase of each nucleus was assigned randomly.

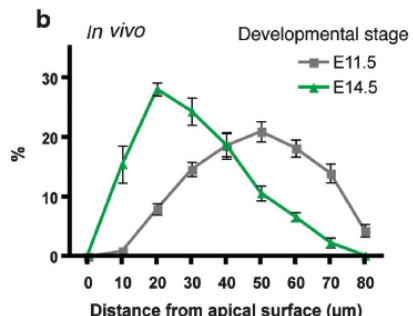
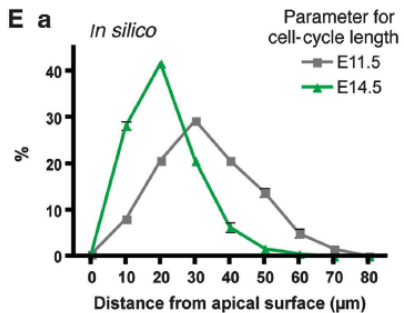
Kosodo et al (2011) EMBO

Kosodo Model: Nuclear Trajectories



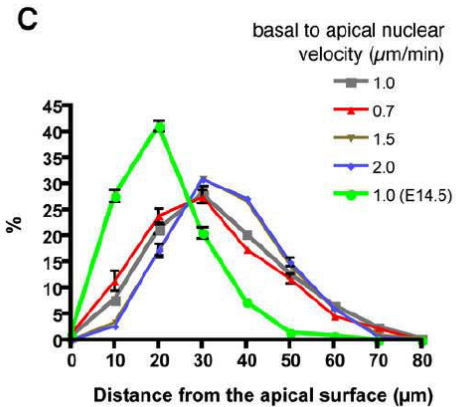
For nuclei in G2- and M-phases, the nuclei were forced to move toward the apical surface with a velocity of $V_{BA} = 1.0 \mu\text{m}/\text{min}$ until they reached the apical surface.

Cell Cycle Length affects nuclear migration



Kosodo et al (2011) EMBO

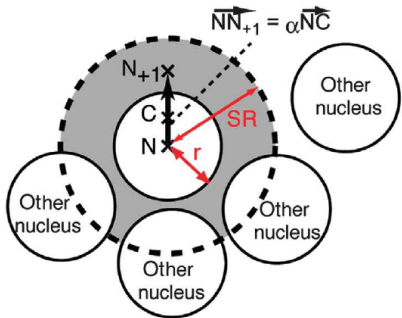
Kosodo Model: G2 Speed of Nuclear Migration does not affect nuclear distribution



Standard velocity of nuclei in G2- and M-phases: $1.0 \mu\text{m}/\text{min}$ until they reach the apical surface.

Cell divisions at M-phase, migration along the radial axis, and volume growth during the cell cycle did not significantly affect apical to basal nuclear migration.

Limitations Kosodo Model (2011) EMBO

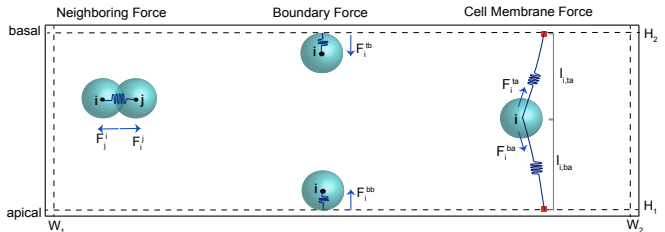
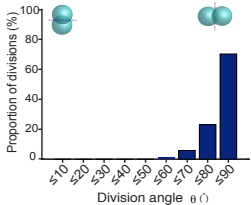
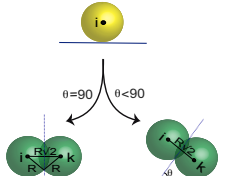


- 2D model: limited "escape trajectories" in 2D
- no physical forces modelled → how do nuclei sense open space?
- comparison of simulated and measured spatial distribution of nuclei → depends mainly on cell cycle length

Open Question

Is there really no impact of nuclear G2 speed, cell divisions, radial migration, and volume growth on the process?

3D Model based on Physical Forces

A**B****C**

Equation of Motion

$$m \frac{d^2 \mathbf{P}_i}{d^2 t} = \sum_i \mathbf{F}_i$$

Nuclei-nuclei Interaction Force

$$\mathbf{F}_i^j = \begin{cases} k_s(d_{i,j} - l_{i,j}) \left(\frac{\mathbf{P}_j - \mathbf{P}_i}{d_{i,j}} \right) & \text{if } d_{i,j} < l_{i,j} \\ \mathbf{0} & \text{if } d_{i,j} \geq l_{i,j} \end{cases}$$
$$\mathbf{F}_i^N = \sum_{j \in \text{neighbors}(i)} \mathbf{F}_i^j$$

Definitions:

- k_s refers to the spring constant.
- $l_{i,j}$ is the resting length of the spring, which is set to the sum of two nuclei radii in the model.
- $d_{i,j} = \|\mathbf{P}_j - \mathbf{P}_i\|$ denotes the Euclidean distance between nuclei i and j .

Boundary Force

$$\mathbf{F}_i^{tb} = \begin{cases} (0, 0, k_{tb}(d_{i,tb} - l_{i,tb})) & \text{if } d_{i,tb} < l_{i,tb} \\ \mathbf{0} & \text{Otherwise} \end{cases}$$

$$\mathbf{F}_i^{bb} = \begin{cases} (0, 0, k_{bb}(d_{i,bb} - l_{i,bb})) & \text{if } d_{i,bb} < l_{i,bb} \\ \mathbf{0} & \text{Otherwise} \end{cases}$$

$$\mathbf{F}_i^b = \mathbf{F}_i^{tb} + \mathbf{F}_i^{bb}$$

k_{tb} and k_{bb} refer to the stiffness constants of the Hookean springs and represent the elasticity of the top and bottom boundaries. \mathbf{F}_i^b is only applied radially, hence, the distances of the nucleus i from the bottom and top boundaries are defined as $d_{i,bb} := z_i - H_1$ and $d_{i,tb} := z_i - H_2$, respectively. The resting lengths of both springs, $l_{i,bb}$ and $l_{i,tb}$, are set to one nucleus radius.

Cell Membrane Force

$$\mathbf{F}_i^{ta} := \begin{cases} k_{ta}(d_{i,ta} - l_{i,ta}) \left(\frac{\mathbf{P}_{i,ta} - \mathbf{P}_i}{d_{i,ta}} \right) & \text{if } d_{i,ta} > l_{i,ta} \\ \mathbf{0} & \text{Otherwise} \end{cases}, \quad (17)$$

$$\mathbf{F}_i^{ba} := \begin{cases} k_{ba}(d_{i,ba} - l_{i,ba}) \left(\frac{\mathbf{P}_{i,ba} - \mathbf{P}_i}{d_{i,ba}} \right) & \text{if } d_{i,ba} > l_{i,ba} \\ \mathbf{0} & \text{Otherwise} \end{cases}, \quad (18)$$

$$\mathbf{F}_i^a = \mathbf{F}_i^{ta} + \mathbf{F}_i^{ba}. \quad (19)$$

k_{ta} and k_{ba} : spring constants for nucleus \leftrightarrow apical / basal membrane.

$l_{i,ta} := |z_{i,0} - H_2|$ and $l_{i,ba} := |z_{i,0} - H_1|$: initial Euclidian distance of nucleus to apical and basal membrane.

$d_{i,ta} := ||\mathbf{P}_{i,ta} - \mathbf{P}_i||$ and $d_{i,ba} := ||\mathbf{P}_{i,ba} - \mathbf{P}_i||$: Euclidean distances between the nucleus and the apical / basal membrane.

$\mathbf{P}_{i,ta} := (x_{i,0}, y_{i,0}, H_2)$ and $\mathbf{P}_{i,ba} := (x_{i,0}, y_{i,0}, H_1)$: anchor positions at apical and basal membranes.

Viscous Drag Force

The nuclei are immersed in the cell cytoplasm. Due to the movement through a viscous fluid, in addition to the active and passive forces, a frictional force acts on the nucleus.

For the typical nuclear size, $L = 10 \mu\text{m}$, nuclear speed, $U = 0.3 \frac{\mu\text{m}}{\text{s}}$, and the reported kinematic viscosity of the cytoplasm, $\nu \in [10^7, 10^{11}] \frac{\mu\text{m}^2}{\text{s}}$, we have as Reynolds number,

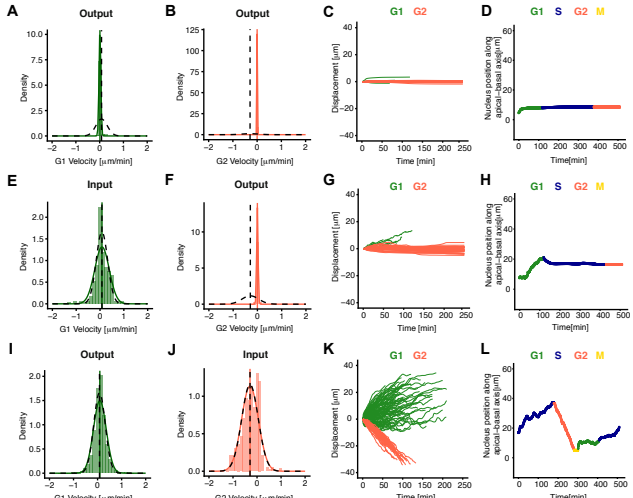
$$Re = \frac{UL}{\nu} \ll 1. \quad (20)$$

For such a small Reynolds number, the viscous drag force can be estimated by Stokes' law,

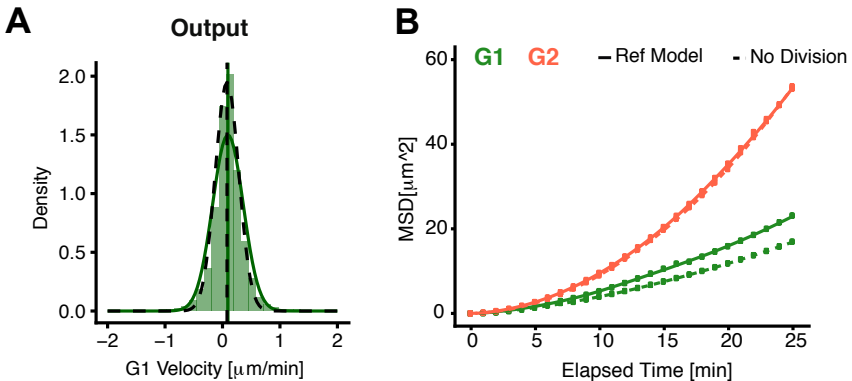
$$\mathbf{F}_i^d := -6\pi\mu R \frac{d\mathbf{P}_i}{dt}. \quad (21)$$

$R = 5 \mu\text{m}$ refers to the nuclear radius, and $\mu \in [10^{-2}, 10^2] \text{ Pa}\cdot\text{s}$ to the viscosity of the cytoplasm.

Active Movement in G2 phase necessary & sufficient to explain zebrafish data

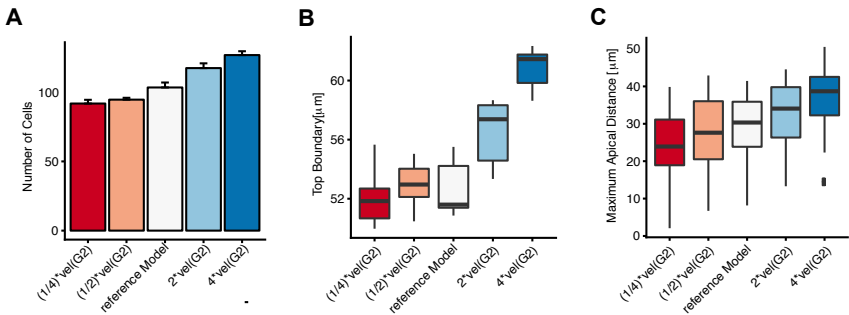


Impact of Cell Division



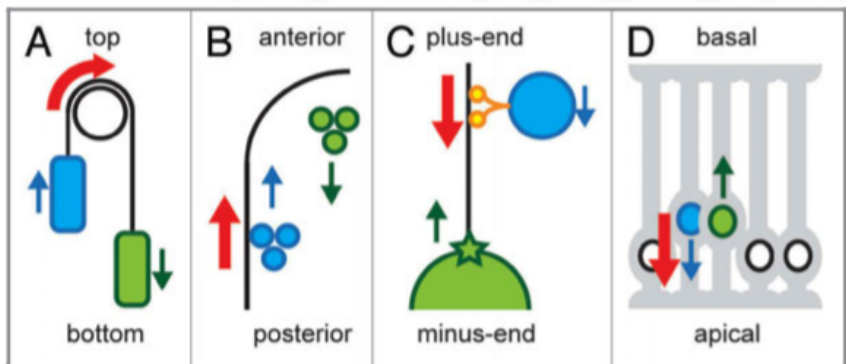
Cell Division without growth increases nuclear density and increases G1 speed of nuclei.

Impact of Nuclear Speed



Higher speed results in widening of apical-basal nuclear distribution.

Cellular Funicular



Niwayama & Kimura (2012) Worm

Literature

- Rivier, N. and A. Lissowski (1982). "On the Correlation between Sizes and Shapes of Cells in Epithelial Mosaics." *J. Phys A: Math. Gen.* 15(3): L143-L148.
- Weliky, M. and G. Oster (1990). "The mechanical basis of cell rearrangement. I. Epithelial morphogenesis during Fundulus epiboly." *Development* 109: 373-386
- Gibson, M. C., et al (2006) The emergence of geometric order in proliferating metazoan epithelia. *Nature* 442, 1038-1041
- Farhadifar, R., et al. (2007). "The influence of cell mechanics, cell-cell interactions, and proliferation on epithelial packing." *Curr Biol* 17(24): 2095-2104.
- Gibson, W. T., et al. (2011). "Control of the mitotic cleavage plane by local epithelial topology." *Cell* 144(3): 427-438.
- Ishihara, S. & Sugimura, K. (2012) Bayesian inference of force dynamics during morphogenesis. *J Theor Biol* 313, 201-211
- Brodland, G. W. et al. (2014) CellFIT: A Cellular Force-Inference Toolkit Using Curvilinear Cell Boundaries. *Plos One* 9

Thanks!!

Thanks for your attention!

Slides for this talk will be available at:

<http://www.bsse.ethz.ch/cobi/education>